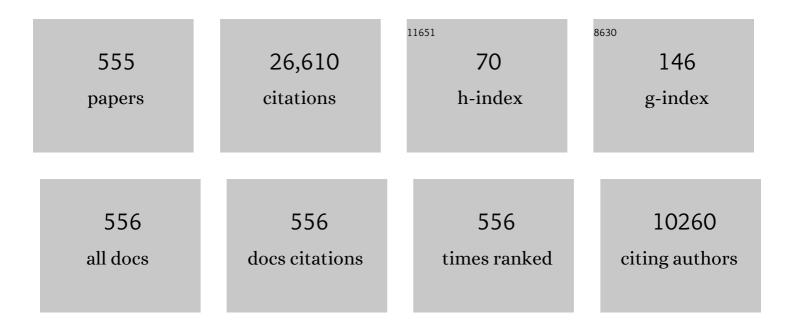
Dingyuan Tang

List of Publications by Year in descending order

Source: https://exaly.com/author-pdf/4621626/publications.pdf Version: 2024-02-01



#	Article	IF	CITATIONS
1	Atomic‣ayer Graphene as a Saturable Absorber for Ultrafast Pulsed Lasers. Advanced Functional Materials, 2009, 19, 3077-3083.	14.9	2,310
2	Molybdenum disulfide (MoS_2) as a broadband saturable absorber for ultra-fast photonics. Optics Express, 2014, 22, 7249.	3.4	1,008
3	Broadband graphene polarizer. Nature Photonics, 2011, 5, 411-415.	31.4	961
4	Mechanically exfoliated black phosphorus as a new saturable absorber for both Q-switching and Mode-locking laser operation. Optics Express, 2015, 23, 12823.	3.4	866
5	Broadband nonlinear optical response in multi-layer black phosphorus: an emerging infrared and mid-infrared optical material. Optics Express, 2015, 23, 11183.	3.4	628
6	Mechanism of multisoliton formation and soliton energy quantization in passively mode-locked fiber lasers. Physical Review A, 2005, 72, .	2.5	587
7	Ultra-short pulse generation by a topological insulator based saturable absorber. Applied Physics Letters, 2012, 101, 211106.	3.3	551
8	Large energy mode locking of an erbium-doped fiber laser with atomic layer graphene. Optics Express, 2009, 17, 17630.	3.4	512
9	Transparent ceramics: Processing, materials and applications. Progress in Solid State Chemistry, 2013, 41, 20-54.	7.2	473
10	Graphene mode locked, wavelength-tunable, dissipative soliton fiber laser. Applied Physics Letters, 2010, 96, .	3.3	456
11	Large energy soliton erbium-doped fiber laser with a graphene-polymer composite mode locker. Applied Physics Letters, 2009, 95, .	3.3	450
12	Monolayer graphene as a saturable absorber in a mode-locked laser. Nano Research, 2011, 4, 297-307.	10.4	408
13	Wavelength-tunable picosecond soliton fiber laser with Topological Insulator: Bi_2Se_3 as a mode locker. Optics Express, 2012, 20, 27888.	3.4	406
14	Dissipative soliton resonance in an all-normaldispersion erbium-doped fiber laser. Optics Express, 2009, 17, 5580.	3.4	310
15	Two-Dimensional CH ₃ NH ₃ PbI ₃ Perovskite Nanosheets for Ultrafast Pulsed Fiber Lasers. ACS Applied Materials & Interfaces, 2017, 9, 12759-12765.	8.0	296
16	Recent progress of study on optical solitons in fiber lasers. Applied Physics Reviews, 2019, 6, .	11.3	295
17	Observation of bound states of solitons in a passively mode-locked fiber laser. Physical Review A, 2001, 64, .	2.5	292
18	Third order nonlinear optical property of Bi 2Se 3. Optics Express, 2013, 21, 2072.	3.4	271

#	Article	IF	CITATIONS
19	Gain-guided soliton in a positive group-dispersion fiber laser. Optics Letters, 2006, 31, 1788.	3.3	244
20	Mode locking of ceramic Nd:yttrium aluminum garnet with graphene as a saturable absorber. Applied Physics Letters, 2010, 96, .	3.3	234
21	Dissipative soliton operation of an ytterbium-doped fiber laser mode locked with atomic multilayer graphene. Optics Letters, 2010, 35, 3622.	3.3	230
22	Observation of High-Order Polarization-Locked Vector Solitons in a Fiber Laser. Physical Review Letters, 2008, 101, 153904.	7.8	226
23	Materials development and potential applications of transparent ceramics: A review. Materials Science and Engineering Reports, 2020, 139, 100518.	31.8	221
24	Few-layer black phosphorus based saturable absorber mirror for pulsed solid-state lasers. Optics Express, 2015, 23, 22643.	3.4	220
25	Multi-wavelength dissipative soliton operation of an erbium-doped fiber laser. Optics Express, 2009, 17, 12692.	3.4	218
26	Compact graphene mode-locked wavelength-tunable erbium-doped fiber lasers: from all anomalous dispersion to all normal dispersion. Laser Physics Letters, 0, 7, 591-596.	1.4	214
27	Soliton interaction in a fiber ring laser. Physical Review E, 2005, 72, 016616.	2.1	210
28	Large Energy, Wavelength Widely Tunable, Topological Insulator Q-Switched Erbium-Doped Fiber Laser. IEEE Journal of Selected Topics in Quantum Electronics, 2014, 20, 315-322.	2.9	201
29	Vector soliton fiber laser passively mode locked by few layer black phosphorus-based optical saturable absorber. Optics Express, 2016, 24, 25933.	3.4	200
30	Soliton collapse and bunched noise-like pulse generation in a passively mode-locked fiber ring laser. Optics Express, 2005, 13, 2289.	3.4	195
31	Graphene mode-locked femtosecond laser at 2Âμm wavelength. Optics Letters, 2012, 37, 2085.	3.3	167
32	Critical coupling with graphene-based hyperbolic metamaterials. Scientific Reports, 2014, 4, 5483.	3.3	158
33	Dark pulse emission of a fiber laser. Physical Review A, 2009, 80, .	2.5	157
34	Review of mid-infrared mode-locked laser sources in the 2.0 <i>μ</i> m–3.5 <i>μ</i> m spectral region. Applied Physics Reviews, 2019, 6, .	11.3	153
35	Dissipative soliton generation in Yb-fiber laser with an invisible intracavity bandpass filter. Optics Letters, 2010, 35, 2756.	3.3	151
36	Noise-like pulse in a gain-guided soliton fiber laser. Optics Express, 2007, 15, 2145.	3.4	148

#	Article	IF	CITATIONS
37	Ultrathin 2D Transition Metal Carbides for Ultrafast Pulsed Fiber Lasers. ACS Photonics, 2018, 5, 1808-1816.	6.6	148
38	Self-Assembled Topological Insulator: Bi\$_{2}\$Se\$_{3}\$ Membrane as a Passive Q-Switcher in an Erbium-Doped Fiber Laser. Journal of Lightwave Technology, 2013, 31, 2857-2863.	4.6	147
39	Coherent energy exchange between components of a vector soliton in fiber lasers. Optics Express, 2008, 16, 12618.	3.4	144
40	Graphene saturable absorber for Q-switching and mode locking at 2 μm wavelength [Invited]. Optical Materials Express, 2012, 2, 878.	3.0	143
41	Vector dissipative solitons in graphene mode locked fiber lasers. Optics Communications, 2010, 283, 3334-3338.	2.1	138
42	Mechanism of intrinsic wavelength tuning and sideband asymmetry in a passively mode-locked soliton fiber ring laser. Journal of the Optical Society of America B: Optical Physics, 2000, 17, 28.	2.1	137
43	Vector dark domain wall solitons in a fiber ring laser. Optics Express, 2010, 18, 4428.	3.4	135
44	Vector multi-soliton operation and interaction in a graphene mode-locked fiber laser. Optics Express, 2013, 21, 10010.	3.4	135
45	Topological Insulator: <formula formulatype="inline"><tex Notation="TeX">\$hbox{Bi}_{2}hbox{Te}_{3}\$ </tex </formula> Saturable Absorber for the Passive Q-Switching Operation of an in-Band Pumped 1645-nm Er:YAG Ceramic Laser. IEEE Photonics Journal, 2013, 5, 1500707-1500707.	2.0	132
46	Dissipative vector solitons in a dispersionmanaged cavity fiber laser with net positive cavity dispersion. Optics Express, 2009, 17, 455.	3.4	130
47	Soliton trapping in fiber lasers. Optics Express, 2008, 16, 9528.	3.4	127
48	Dual-wavelength synchronously mode-locked Nd:CNGG laser. Optics Letters, 2008, 33, 1872.	3.3	126
49	Polarization rotation vector solitons in a graphene mode-locked fiber laser. Optics Express, 2012, 20, 27283.	3.4	118
50	Mechanism of Dissipative-Soliton-Resonance Generation in Passively Mode-Locked All-Normal-Dispersion Fiber Lasers. Journal of Lightwave Technology, 2015, 33, 3781-3787.	4.6	112
51	Generation of 47-fs pulses directly from an erbium-doped fiber laser. Optics Letters, 2007, 32, 41.	3.3	107
52	Bound-soliton fiber laser. Physical Review A, 2002, 66, .	2.5	99
53	Induced solitons formed by cross-polarization coupling in a birefringent cavity fiber laser. Optics Letters, 2008, 33, 2317.	3.3	96
54	Generation of 15-nJ bunched noise-like pulses with 93-nm bandwidth in an erbium-doped fiber ring laser. Applied Physics B: Lasers and Optics, 2006, 83, 553-557.	2.2	94

#	Article	IF	CITATIONS
55	9.2â€₩ diode–end–pumped Yb:Y2O3 ceramic laser. Applied Physics Letters, 2005, 86, 161116.	3.3	91
56	Subpicosecond pulse generation from a Nd:CLNGG disordered crystal laser. Optics Letters, 2009, 34, 103.	3.3	91
57	120nm Bandwidth noise-like pulse generation in an erbium-doped fiber laser. Optics Communications, 2008, 281, 157-161.	2.1	86
58	Polarization rotation locking of vector solitons in a fiber ring laser. Optics Express, 2008, 16, 10053.	3.4	85
59	Coexistence and interaction of vector and bound vector solitons in a dispersion-managed fiber laser mode locked by graphene. Optics Express, 2016, 24, 1814.	3.4	85
60	Stimulated soliton pulse formation and its mechanism in a passively mode-locked fibre soliton laser. Optics Communications, 1999, 165, 189-194.	2.1	83
61	Supercapacitance of Solid Carbon Nanofibers Made from Ethanol Flames. Journal of Physical Chemistry C, 2008, 112, 3612-3618.	3.1	83
62	Observation of polarization domain wall solitons in weakly birefringent cavity fiber lasers. Physical Review B, 2009, 80, .	3.2	83
63	Bound states of solitons in a fiber laser mode locked with carbon nanotube saturable absorber. Optics Communications, 2011, 284, 3615-3618.	2.1	82
64	Dual-wavelength domain wall solitons in a fiber ring laser. Optics Express, 2011, 19, 3525.	3.4	81
65	Generation of 30  fs pulses from a diode-pumped graphene mode-locked Yb:CaYAlO_4 laser. Optics Letters, 2016, 41, 890.	3.3	80
66	Diode-pumped Yb:Y2O3 ceramic laser. Applied Physics Letters, 2003, 82, 2556-2558.	3.3	79
67	Observation of period-doubling bifurcations in a femtosecond fiber soliton laser with dispersion management cavity. Optics Express, 2004, 12, 4573.	3.4	75
68	High-power self-mode-locked Yb:Y_2O_3 ceramic laser. Optics Letters, 2007, 32, 2741.	3.3	75
69	Low Loss, High <scp>NA</scp> Chalcogenide Glass Fibers for Broadband Midâ€Infrared Supercontinuum Generation. Journal of the American Ceramic Society, 2015, 98, 1389-1392.	3.8	75
70	Ga–Sb–S Chalcogenide Glasses for Midâ€Infrared Applications. Journal of the American Ceramic Society, 2016, 99, 12-15.	3.8	75
71	Engineered surface Bloch waves in graphene-based hyperbolic metamaterials. Optics Express, 2014, 22, 3054.	3.4	73
72	Tunable optical bistability at the graphene-covered nonlinear interface. Applied Physics Letters, 2014, 104, .	3.3	72

#	Article	IF	CITATIONS
73	Bound states of dispersion-managed solitons in a fiber laser at near zero dispersion. Applied Optics, 2007, 46, 4768.	2.1	69
74	Coexistence of polarization-locked and polarization-rotating vector solitons in a fiber laser with SESAM. Optics Letters, 2009, 34, 3059.	3.3	69
75	The effect of MgO and SiO2 codoping on the properties of Nd:YAG transparent ceramic. Optical Materials, 2012, 34, 940-943.	3.6	65
76	Room temperature continuous-wave laser performance of LD pumped Er:Lu_2O_3 and Er:Y_2O_3 ceramic at 27 μm. Optics Express, 2014, 22, 19495.	3.4	65
77	High-efficiency 1040 and 1078 nm laser emission of a Yb:Y_2O_3 ceramic laser with 976 nm diode pumping. Optics Letters, 2007, 32, 247.	3.3	64
78	Generation of 534 fs pulses from a passively mode-locked Nd:CLNGG-CNGG disordered crystal hybrid laser. Laser Physics Letters, 2010, 7, 483-486.	1.4	64
79	Characterization and compression of dissipative-soliton-resonance pulses in fiber lasers. Scientific Reports, 2016, 6, 23631.	3.3	62
80	Dual-wavelength passively mode-locked Nd:LuYSiO_5 laser with SESAM. Optics Express, 2011, 19, 3984.	3.4	61
81	Diode-end-pumped 42-W continuous-wave Yb:Y_2O_3 ceramic laser. Optics Letters, 2004, 29, 1212.	3.3	60
82	High-power continuous wave and passively Q-switched laser operations of a Nd:GGG crystal. Laser Physics Letters, 2008, 5, 100-103.	1.4	60
83	Agglomeration Control of Nd:YAG Nanoparticles Via Freeze Drying for Transparent Nd:YAG Ceramics. Journal of the American Ceramic Society, 2009, 92, 812-817.	3.8	59
84	Bunch of restless vector solitons in a fiber laser with SESAM. Optics Express, 2009, 17, 8103.	3.4	59
85	In-band pumped highly efficient Ho:YAG ceramic laser with 21 W output power at 2097 nm. Optics Letters, 2011, 36, 1575.	3.3	59
86	Discrete wavelength tunable laser using microelectromechanical systems technology. Applied Physics Letters, 2004, 84, 329-331.	3.3	58
87	High-power passive mode locking of a compact diode-pumped Nd:LuVO ₄ laser. Laser Physics Letters, 2008, 5, 647-650.	1.4	58
88	On-chip photonic Fourier transform with surface plasmon polaritons. Light: Science and Applications, 2016, 5, e16034-e16034.	16.6	58
89	Dissipative soliton trapping in normal dispersion-fiber lasers. Optics Letters, 2010, 35, 1902.	3.3	57
90	Highly efficient 2 μm Tm:YAG ceramic laser. Optics Letters, 2012, 37, 1076.	3.3	57

#	Article	IF	CITATIONS
91	Dynamics of gain-guided solitons in an all-normal-dispersion fiber laser. Optics Letters, 2007, 32, 1806.	3.3	55
92	Toward vacuum sintering of YAG transparent ceramic using divalent dopant as sintering aids: Investigation of microstructural evolution and optical property. Ceramics International, 2017, 43, 3140-3146.	4.8	55
93	Generation of femtosecond optical vortices using a single refractive optical element. Applied Physics Letters, 2006, 88, 091103.	3.3	53
94	Soliton polarization dynamics in fiber lasers passively mode-locked by the nonlinear polarization rotation technique. Physical Review E, 2006, 74, 046605.	2.1	53
95	Highly efficient Tm:YAG ceramic laser resonantly pumped at 1617 nm. Optics Letters, 2011, 36, 4485.	3.3	53
96	Evidence of dark solitons in all-normal-dispersion-fiber lasers. Physical Review A, 2013, 88, .	2.5	52
97	Dark soliton fiber lasers. Optics Express, 2014, 22, 19831.	3.4	51
98	Diode-pumped passively mode-locked Nd:GdVO4 laser with a GaAs saturable absorber mirror. Applied Physics B: Lasers and Optics, 2004, 79, 203-206.	2.2	50
99	Fabrication and laser properties of transparent Yb:YAG ceramics. Optical Materials, 2012, 34, 936-939.	3.6	50
100	Passively Q-switched Yb:YAG laser with a GaAs output coupler. Optics Communications, 2002, 211, 271-275.	2.1	49
101	Cavity-birefringence-dependent h-shaped pulse generation in a thulium-holmium-doped fiber laser. Optics Letters, 2018, 43, 247.	3.3	49
102	Generation of multiple gain-guided solitons in a fiber laser. Optics Letters, 2007, 32, 1581.	3.3	48
103	Bound states of gain-guided solitons in a passively mode-locked fiber laser. Optics Letters, 2007, 32, 3191.	3.3	48
104	Characterization of laser crystal Yb:CaYAlO_4. Journal of the Optical Society of America B: Optical Physics, 2011, 28, 1650.	2.1	48
105	Fabrication of transparent ZnS ceramic by optimizing the heating rate in spark plasma sintering process. Optical Materials, 2015, 50, 36-39.	3.6	48
106	Short pulse passively Q-switched Nd:GdYVO4 laser using a GaAs mirror. Optics Communications, 2006, 259, 256-260.	2.1	47
107	Nanosecond square pulse generation in fiber lasers with normal dispersion. Optics Communications, 2007, 272, 431-434.	2.1	47
108	Mapping plasmonic near-field profiles and interferences by surface-enhanced Raman scattering. Scientific Reports, 2013, 3, 3064.	3.3	47

#	Article	lF	CITATIONS
109	Light-emission properties in nanocrystalline BaTiO3. Applied Physics Letters, 2000, 77, 2807-2809.	3.3	46
110	Deterministic chaos in a diode-pumped Nd:YAG laser passively Q switched by a Cr^4+:YAG crystal. Optics Letters, 2003, 28, 325.	3.3	46
111	Group-velocity-locked vector soliton molecules in fiber lasers. Scientific Reports, 2017, 7, 2369.	3.3	46
112	Observation of generalized synchronization of chaos in a driven chaotic system. Physical Review E, 1998, 57, 5247-5251.	2.1	45
113	Passive harmonic mode locking of twin-pulse solitons in an erbium-doped fiber ring laser. Optics Communications, 2004, 229, 363-370.	2.1	44
114	Multipulse bound solitons with fixed pulse separations formed by direct soliton interaction. Applied Physics B: Lasers and Optics, 2005, 80, 239-242.	2.2	44
115	Mechanism of Spectrum Moving, Narrowing, Broadening, and Wavelength Switching of Dissipative Solitons in All-Normal-Dispersion Yb-Fiber Lasers. IEEE Photonics Journal, 2014, 6, 1-8.	2.0	44
116	Manipulation of Group-Velocity-Locked Vector Solitons From Fiber Lasers. IEEE Photonics Journal, 2016, 8, 1-6.	2.0	44
117	Gain-guided solitons in dispersion-managed fiber lasers with large net cavity dispersion. Optics Letters, 2006, 31, 2957.	3.3	43
118	Diode-pumped passively mode-locked Nd:CTGG disordered crystal laser. Applied Physics B: Lasers and Optics, 2009, 95, 691-695.	2.2	43
119	Systematic optimization of spray drying for YAG transparent ceramics. Journal of the European Ceramic Society, 2015, 35, 2391-2401.	5.7	43
120	Type-III intermittency of a laser. Physical Review A, 1991, 44, R35-R38.	2.5	42
121	Passive femtosecond mode-locking and cw laser performance of Yb^3+: Sc_2SiO_5. Optics Express, 2010, 18, 16739.	3.4	42
122	A resonantly-pumped tunable Q-switched Ho:YAG ceramic laser with diffraction-limit beam quality. Optics Express, 2014, 22, 254.	3.4	42
123	Effects of Sintering Aids on the Transparency and Conversion Efficiency of Cr 4+ Ions in Cr: YAG Transparent Ceramics. Journal of the American Ceramic Society, 2015, 98, 2459-2464.	3.8	41
124	Bound soliton pulses in passively mode-locked fiber laser. Optics Communications, 2001, 200, 389-399.	2.1	40
125	Compound pulse solitons in a fiber ring laser. Physical Review A, 2003, 68, .	2.5	40
126	Tunable laser using micromachined grating with continuous wavelength tuning. Applied Physics Letters, 2004, 85, 3684-3686.	3.3	40

#	Article	IF	CITATIONS
127	Dy3+-doped Ga–Sb–S chalcogenide glasses for mid-infrared lasers. Materials Research Bulletin, 2015, 70, 55-59.	5.2	40
128	Hollow-core air-gap anti-resonant fiber couplers. Optics Express, 2017, 25, 29296.	3.4	39
129	Pulse-train nonuniformity in a fiber soliton ring laser mode-locked by using the nonlinear polarization rotation technique. Physical Review A, 2004, 69, .	2.5	38
130	Yb:LuAG laser ceramics: a promising high power laser gain medium. Optical Materials Express, 2012, 2, 1425.	3.0	38
131	\$L\$ -Band Femtosecond Fiber Laser Mode Locked by Nonlinear Polarization Rotation. IEEE Photonics Technology Letters, 2014, 26, 2438-2441.	2.5	38
132	Broadband chirality-coded meta-aperture for photon-spin resolving. Nature Communications, 2015, 6, 10051.	12.8	38
133	Spectral characteristics of a Yb-doped Y2O3 ceramic laser. Applied Physics B: Lasers and Optics, 2004, 79, 449-455.	2.2	37
134	Lithium Insertion in Channel-Structured β-AgVO ₃ : <i>In Situ</i> Raman Study and Computer Simulation. Chemistry of Materials, 2007, 19, 5965-5972.	6.7	37
135	Diode-pumped continuous-wave and Q-switched Tm:Y_2O_3 ceramic laser around 2050 nm. Optical Materials Express, 2017, 7, 296.	3.0	37
136	Tunable and switchable harmonic h-shaped pulse generation in a 303  km ultralong mode-locked thulium-doped fiber laser. Photonics Research, 2019, 7, 332.	7.0	37
137	Generation of noise-like pulses with 203 nm 3-dB bandwidth. Optics Express, 2019, 27, 24147.	3.4	37
138	Soliton modulation instability in fiber lasers. Physical Review A, 2009, 80, .	2.5	36
139	Direct laser writing of near-IR step-index buried channel waveguides in rare earth doped YAG. Optics Letters, 2011, 36, 3395.	3.3	36
140	Polycrystalline <scp><scp>Ho:YAG</scp></scp> Transparent Ceramics for Eye afe Solid State Laser Applications. Journal of the American Ceramic Society, 2012, 95, 52-55.	3.8	36
141	Highly transparent Nd^3+:Lu_2O_3 produced by spark plasma sintering and its laser oscillation. Optical Materials Express, 2014, 4, 1420.	3.0	36
142	280  GHz dark soliton fiber laser. Optics Letters, 2014, 39, 3484.	3.3	36
143	Dissipative soliton resonance and its depression into burst-like emission in a holmium-doped fiber laser with large normal dispersion. Optics Letters, 2019, 44, 2414.	3.3	36
144	Passively Q-switched Yb:Y2O3 ceramic laser with a GaAs output coupler. Optics Express, 2004, 12, 3560.	3.4	35

#	Article	IF	CITATIONS
145	Continuous wavelength tuning in micromachined Littrow external-cavity lasers. IEEE Journal of Quantum Electronics, 2005, 41, 187-197.	1.9	35
146	Passive mode-locking performance with a mixed Nd:Lu_05Gd_05VO_4 crystal. Optics Express, 2009, 17, 3264.	3.4	34
147	Observation of dip-type sidebands in a soliton fiber laser. Optics Communications, 2010, 283, 340-343.	2.1	34
148	Emission pattern of surface-enhanced Raman scattering from single nanoparticle-film junction. Applied Physics Letters, 2013, 102, .	3.3	33
149	Polarization Domain Formation and Domain Dynamics in a Quasi-Isotropic Cavity Fiber Laser. IEEE Journal of Selected Topics in Quantum Electronics, 2014, 20, 42-50.	2.9	33
150	All-fiber short-wavelength tunable mode-locked fiber laser using normal dispersion thulium-doped fiber. Optics Express, 2020, 28, 17570.	3.4	33
151	Passive mode locking of a diode-pumped Nd:Cd 0.64 Y 0.36 VO 4 laser with a GaAs saturable absorber mirror. Applied Physics B: Lasers and Optics, 2005, 80, 475-477.	2.2	32
152	Tightly Focused Radially Polarized Beam for Propagating Surface Plasmon-Assisted Gap-Mode Raman Spectroscopy. Plasmonics, 2011, 6, 651-657.	3.4	32
153	Edge-reflection phase directed plasmonic resonances on graphene nano-structures. Optics Express, 2014, 22, 22689.	3.4	32
154	Ga ₂ S ₃ ‣b ₂ S ₃ si chalcohalide glasses for midâ€infrared applications. Journal of the American Ceramic Society, 2017, 100, 5107-5112.	3.8	32
155	Subsideband generation and modulational instability lasing in a fiber soliton laser. Journal of the Optical Society of America B: Optical Physics, 2001, 18, 1443.	2.1	31
156	Bound twin-pulse solitons in a fiber ring laser. Physical Review E, 2004, 70, 067602.	2.1	31
157	Regimes of operation states in passively mode-locked fiber soliton ring laser. Optics and Laser Technology, 2004, 36, 299-307.	4.6	31
158	Quasi-cw diode-pumped Nd:GdVO4 laser passively Q-switched and mode-locked by Cr4+:YAG saturable absorber. Optics Communications, 2005, 250, 168-173.	2.1	31
159	Diode-end-pumped passively mode-locked Nd:GGG laser with a semiconductor saturable mirror. Optics Communications, 2008, 281, 4762-4764.	2.1	31
160	Vector Soliton Generation in a Tm Fiber Laser. IEEE Photonics Technology Letters, 2014, 26, 769-772.	2.5	31
161	Raman-scattering-assistant broadband noise-like pulse generation in all-normal-dispersion fiber lasers. Optics Express, 2015, 23, 25889.	3.4	31
162	Mode-locking of fiber lasers induced by residual polarization dependent loss of cavity components. Laser Physics, 2010, 20, 1913-1917.	1.2	30

#	Article	IF	CITATIONS
163	High-power polycrystalline Er:YAG ceramic laser at 1617 nm. Optics Letters, 2011, 36, 4767.	3.3	30
164	Yb:Y 2 O 3 transparent ceramics processed with hot isostatic pressing. Optical Materials, 2017, 71, 117-120.	3.6	30
165	Fabrication and spectral properties of Dy:Y2O3 transparent ceramics. Journal of the European Ceramic Society, 2018, 38, 1981-1985.	5.7	30
166	Fabrication of Er:Y2O3 transparent ceramics for 2.7â€Î¼m mid-infrared solid-state lasers. Journal of the European Ceramic Society, 2020, 40, 444-448.	5.7	30
167	Various soliton molecules in fiber systems. Applied Optics, 2019, 58, 2745.	1.8	30
168	Chaotic dynamics of a passively mode-locked soliton fiber ring laser. Chaos, 2006, 16, 013128.	2.5	29
169	Coexistence and competition between different soliton-shaping mechanisms in a laser. Physical Review A, 2007, 75, .	2.5	29
170	Femtosecond and continuous-wave laser performance of a diode-pumped Yb^3+:CaYAlO_4 laser. Optics Letters, 2011, 36, 259.	3.3	29
171	Diode-end-pumped Nd:CaYAlO4 mode locked laser. Optics Communications, 2011, 284, 1967-1969.	2.1	29
172	High-resolution chalcogenide fiber bundles for infrared imaging. Optics Letters, 2015, 40, 4384.	3.3	29
173	Period-Doubling and Quadrupling Bifurcation of Vector Soliton Bunches in a Graphene Mode Locked Fiber Laser. IEEE Photonics Journal, 2017, 9, 1-8.	2.0	29
174	Models, predictions, and experimental measurements of far-infrared NH3-laser dynamics and comparisons with the Lorenz-Haken model. Applied Physics B: Lasers and Optics, 1995, 61, 223-242.	2.2	28
175	High power passively Q-switched Nd:GdVO4 lasers. Optics Communications, 2004, 229, 331-336.	2.1	28
176	Effect of grain size on the sinterability of yttria nanopowders synthesized by carbonate-precipitation process. Materials Chemistry and Physics, 2008, 112, 423-426.	4.0	28
177	Fabrication and properties of highly transparent Er:YAG ceramics. Optical Materials, 2012, 34, 973-976.	3.6	28
178	A graphene-based passively <i>Q</i> -switched polycrystalline Er:YAG ceramic laser operating at 1645 nm. Laser Physics Letters, 2013, 10, 055801.	1.4	28
179	Fabrication and characterization of highly transparent Yb3+: Y2O3 ceramics. Optical Materials, 2015, 50, 21-24.	3.6	28
180	Improved conversion efficiency of Cr4+ ions in Cr: YAG transparent ceramics by optimization the particle sizes of sintering aids. Optical Materials, 2015, 50, 11-14.	3.6	28

#	Article	IF	CITATIONS
181	Synchronization of mutually coupled chaotic systems. Physical Review E, 1997, 55, 6618-6623.	2.1	27
182	Passively mode-locked Nd:LuVO_4 laser with a GaAs wafer. Optics Letters, 2008, 33, 225.	3.3	27
183	Diode pumped and mode-locked Yb:CdYAG ceramic lasers. Laser Physics Letters, 2011, 8, 719-722.	1.4	27
184	Efficient RTP-based OPO intracavity pumped by an acousto-optic Q-switched Nd:YVO_4 laser. Optics Letters, 2014, 39, 1314.	3.3	27
185	Pump laser induced photodarkening in ZrO2-doped Yb:Y2O3 laser ceramics. Journal of the European Ceramic Society, 2019, 39, 635-640.	5.7	27
186	Nonlinear Absorbing-Loop Mirror in a Holmium-Doped Fiber Laser. Journal of Lightwave Technology, 2020, 38, 6069-6075.	4.6	27
187	Field dynamics of a single-mode laser. Physical Review A, 1991, 44, 7597-7604.	2.5	26
188	Period-doubling and quadrupling of bound solitons in a passively mode-locked fiber laser. Optics Communications, 2005, 252, 167-172.	2.1	26
189	Dual-wavelength single-longitudinal-mode erbium-doped fiber laser based on inverse-Gaussian apodized fiber Bragg grating and its application in microwave generation. Optical Fiber Technology, 2011, 17, 120-123.	2.7	26
190	Densification and microstructural evolution of yttria transparent ceramics: The effect of ball milling conditions. Journal of the European Ceramic Society, 2015, 35, 1011-1019.	5.7	26
191	Diode-pumped high power 2.7Âμm Er:Y 2 O 3 ceramic laser at room temperature. Optical Materials, 2017, 71, 70-73.	3.6	26
192	Generation of sub-50fs soliton pulses from a mode-locked Yb,Na:CNGG disordered crystal laser. Optics Express, 2017, 25, 14968.	3.4	26
193	Observation of dark-bright vector solitons in fiber lasers. Optics Letters, 2019, 44, 2185.	3.3	26
194	Experimental study of a high-power CW side-pumped Nd:YAG laser. Optics and Laser Technology, 2003, 35, 37-42.	4.6	25
195	Period-doubling of gain-guided solitons in fiber lasers of large net normal dispersion. Optics Communications, 2008, 281, 3557-3560.	2.1	25
196	Ultrahigh-repetition-rate bound-soliton fiber laser. Applied Physics B: Lasers and Optics, 2010, 99, 441-447.	2.2	25
197	Mechanism for stable, ultra-flat multiwavelength operation in erbium-doped fiber lasers employing intensity-dependent loss. Optics and Laser Technology, 2012, 44, 74-77.	4.6	25
198	GHz pulse train generation in fiber lasers by cavity induced modulation instability. Optical Fiber Technology, 2014, 20, 610-614.	2.7	25

#	Article	IF	CITATIONS
199	Laser dynamics of type-I intermittency. Physical Review A, 1992, 46, 676-678.	2.5	24
200	Modulational instability in a fiber soliton ring laser induced by periodic dispersion variation. Physical Review A, 2000, 61, .	2.5	24
201	Q-switched and continuous-wave mode-locking of a diode-pumped Nd:Gd0.64Y0.36VO4â^'Cr4+:YAG laser. Applied Physics B: Lasers and Optics, 2005, 81, 511-515.	2.2	24
202	Temperature-tunable nanosecond optical parametric oscillator based on periodically poled. Optics and Laser Technology, 2006, 38, 192-195.	4.6	24
203	Passive harmonic mode locking of soliton bunches in a fiber ring laser. Optical and Quantum Electronics, 2008, 40, 1053-1064.	3.3	24
204	High-power mode-locked operation of Yb-doped NaY(WO ₄) ₂ end-pumped by laser diodes. Laser Physics Letters, 2008, 5, 651-654.	1.4	24
205	Synthesis and characterization of yttrium aluminum garnet by high-energy ball milling. Optical Materials, 2009, 31, 716-719.	3.6	24
206	Gain dispersion for dissipative soliton generation in all-normal-dispersion fiber lasers. Applied Optics, 2009, 48, 5131.	2.1	24
207	Fabrication and plasma resistance properties of transparent YAG ceramics. Ceramics International, 2012, 38, 2529-2535.	4.8	24
208	Novel transparent ceramics for solid-state lasers. High Power Laser Science and Engineering, 2013, 1, 138-147.	4.6	24
209	Temporal cavity soliton formation in an anomalous dispersion cavity fiber laser. Journal of the Optical Society of America B: Optical Physics, 2014, 31, 3050.	2.1	24
210	Characterization of spray granulated Nd:YAG particles for transparent ceramics. Journal of Alloys and Compounds, 2015, 639, 244-251.	5.5	24
211	Low temperature-sintering and microstructure of highly transparent yttria ceramics. Journal of Alloys and Compounds, 2017, 695, 2580-2586.	5.5	24
212	Holmium doped yttria transparent ceramics for 2-μm solid state lasers. Journal of the European Ceramic Society, 2018, 38, 1986-1989.	5.7	24
213	Passively mode-locked Yb:Y2O3 ceramic laser with a GaAs-saturable absorber mirror. Optics Communications, 2004, 237, 165-168.	2.1	23
214	High Fundamental Repetition Rate Fiber Lasers Operated in Strong Normal Dispersion Regime. IEEE Photonics Technology Letters, 2009, 21, 724-726.	2.5	23
215	Densification of Yttria Transparent Ceramics: The Utilization of Activated Sintering. Journal of the American Ceramic Society, 2016, 99, 1671-1675.	3.8	23
216	Dissipative Soliton Resonances in a Mode-Locked Holmium-Doped Fiber Laser. IEEE Photonics Technology Letters, 2018, 30, 1699-1702.	2.5	23

#	Article	IF	CITATIONS
217	Sub-five-optical-cycle pulse generation from a Kerr-lens mode-locked Yb:CaYAlO ₄ laser. Optics Letters, 2021, 46, 2328.	3.3	23
218	Satellite Pulse Generation in Diode-Pumped Passively Q-Switched <tex>\$hboxNd:GdVO_4\$</tex> Lasers. IEEE Journal of Quantum Electronics, 2006, 42, 625-632.	1.9	22
219	Period-doubling of vector solitons in a ring fiber laser. Optics Communications, 2008, 281, 5614-5617.	2.1	22
220	Diode-pumped passively Q-switched Nd:GGG crystal with GaAs saturable absorber. Laser Physics, 2008, 18, 719-721.	1.2	22
221	Crystallization kinetics and characterization of nanosized Nd:YAG by a modified sol–gel combustion process. Journal of Crystal Growth, 2013, 362, 52-57.	1.5	22
222	New double-sintering aid for fabrication of highly transparent ytterbium-doped yttria ceramics. Journal of the European Ceramic Society, 2016, 36, 253-256.	5.7	22
223	Spark plasma sintering of Sm3+ doped Y2O3 transparent ceramics for visible light lasers. Ceramics International, 2017, 43, 12057-12060.	4.8	22
224	Ho ³⁺ :Y ₂ O ₃ ceramic laser generated over 113  W of output powe 2117  nm. Optics Letters, 2019, 44, 5933.	er at 3.3	22
225	Deviation from Lorenz-type dynamics of an NH3 ring laser. Optics Communications, 1992, 89, 47-53.	2.1	21
226	Fabrication of yttrium aluminum garnet transparent ceramics from yttria nanopowders synthesized by carbonate precipitation. Journal of Electroceramics, 2009, 23, 89-93.	2.0	21
227	Preparation and upconversion luminescence of YAG(Y3Al5O12): Yb3+, Ho3+ nanocrystals. Journal of Rare Earths, 2009, 27, 66-70.	4.8	21
228	Comparison of the 1319 and 1338 nm Dual-Wavelength Emission of Neodymium-Doped Yttrium Aluminum Garnet Ceramic and Crystal Lasers. Applied Physics Express, 2013, 6, 012701.	2.4	21
229	Dy ³⁺ /Ce ³⁺ Codoped <scp>YAG</scp> Transparent Ceramics for Singleâ€Composition Tunable Whiteâ€Light Phosphor. Journal of the American Ceramic Society, 2015, 98, 3231-3235.	3.8	21
230	Fabrication, optical properties and LD-pumped 2.7μm laser performance of low Er3+ concentration doped Lu2O3 transparent ceramics. Journal of Alloys and Compounds, 2015, 640, 51-55.	5.5	21
231	Efficient laser operation based on transparent Nd:Lu_2O_3 ceramic fabricated by Spark Plasma Sintering. Optics Express, 2016, 24, 20571.	3.4	21
232	Mid-infrared luminescence of Dy3+ ions in modified Ga-Sb-S chalcogenide glasses and fibers. Journal of Alloys and Compounds, 2017, 695, 1237-1242.	5.5	21
233	Submicronâ€grained Yb:Lu ₂ O ₃ transparent ceramics with lasing quality. Journal of the American Ceramic Society, 2019, 102, 2587-2592.	3.8	21
234	Dissipative dark-bright vector solitons in fiber lasers. Physical Review A, 2020, 101, .	2.5	21

#	Article	IF	CITATIONS
235	Lorenz-like chaos in NH3-FIR lasers. Infrared Physics and Technology, 1995, 36, 489-512.	2.9	20
236	Random-wavelength solid-state laser. Optics Letters, 2004, 29, 65.	3.3	20
237	Recoverable Photoluminescence of Flame-Synthesized Multiwalled Carbon Nanotubes and Its Intensity Enhancement at 240 K. Journal of Physical Chemistry C, 2007, 111, 10347-10352.	3.1	20
238	Spark plasma sintering-fabricated one-dimensional nanoscale "crystalline-amorphous―carbon heterojunction. Applied Physics Letters, 2008, 92, 113113.	3.3	20
239	CW laser properties of Nd:GdYAG, Nd:LuYAG, and Nd:GdLuAG mixed crystals. Laser Physics, 2011, 21, 1742-1744.	1.2	20
240	Group velocity locked vector dissipative solitons in a high repetition rate fiber laser. Optics Express, 2016, 24, 18718.	3.4	20
241	Compact self-cascaded KTA-OPO for 26 μm laser generation. Optics Express, 2016, 24, 26529.	3.4	20
242	Sub-80 femtosecond pulses generation from a diode-pumped mode-locked Nd:Ca_3La_2(BO_3)_4 disordered crystal laser. Optics Letters, 2016, 41, 1384.	3.3	20
243	Stable passively harmonic mode-locking dissipative pulses in 2µm solid-state laser. Optics Express, 2017, 25, 1815.	3.4	20
244	Narrow-bandwidth h-shaped pulse generation and evolution in a net normal dispersion thulium-doped fiber laser. Optics Express, 2019, 27, 29770.	3.4	20
245	Synchronization of chaotic laser mode dynamics. Physical Review A, 1996, 54, 5317-5322.	2.5	19
246	Passive mode-locking of a Nd:YAG ceramic laser by optical interference modulation in a GaAs wafer. Optics Express, 2007, 15, 5360.	3.4	19
247	Switchable dual-wavelength single-longitudinal-mode erbium-doped fiber laser using an inverse-Gaussian apodized fiber Bragg grating filter and a low-gain semiconductor optical amplifier. Applied Optics, 2010, 49, 6855.	2.1	19
248	Laser operation of diode-pumped Er,Yb co-doped YAG ceramics at 16 μm. Optics Express, 2013, 21, 26955.	3.4	19
249	The effects of germanium addition on properties of Ga-Sb-S chalcogenide glasses. Journal of Non-Crystalline Solids, 2016, 452, 114-118.	3.1	19
250	Crystal growth and properties of the disordered crystal Yb:SrLaAlO ₄ : a promising candidate for high-power ultrashort pulse lasers. CrystEngComm, 2018, 20, 3388-3395.	2.6	19
251	Internal polarization dynamics of vector dissipative-soliton-resonance pulses in normal dispersion fiber lasers. Optics Letters, 2018, 43, 1222.	3.3	19
252	Fabrication of Highly Transparent Y2O3 Ceramics with CaO as Sintering Aid. Materials, 2021, 14, 444.	2.9	19

#	Article	IF	CITATIONS
253	Observation of incoherently coupled dark-bright vector solitons in single-mode fibers. Optics Express, 2019, 27, 18311.	3.4	19
254	High transparency Pr:Y2O3 ceramics: A promising gain medium for red emission solid-state lasers. Journal of Advanced Ceramics, 2022, 11, 874-881.	17.4	19
255	Experimental evidence of frequency entrainment between coupled chaotic oscillations. Physical Review E, 1998, 57, 3649-3651.	2.1	18
256	Stages of chaotic synchronization. Chaos, 1998, 8, 697-701.	2.5	18
257	Period-doubling of dispersion-managed solitons in an Erbium-doped fiber laser at around zero dispersion. Optics Communications, 2007, 278, 428-433.	2.1	18
258	Efficient operation of a diode-pumped Yb:NaY(WO_4)_2 laser. Optics Express, 2008, 16, 1686.	3.4	18
259	Pulse breaking recovery in fiber lasers. Optics Express, 2008, 16, 12102.	3.4	18
260	Polycrystalline Ceramic Er:YAG Laser In-Band Pumped by a High-Power Er,Yb Fiber Laser at 1532 nm. Applied Physics Express, 2011, 4, 052701.	2.4	18
261	Evidence of dissipative solitons in Yb^3+:CaYAlO_4. Optics Express, 2011, 19, 18495.	3.4	18
262	High-efficiency diode-pumped Tm:YAG ceramic laser. Optical Materials, 2013, 35, 804-806.	3.6	18
263	Generation of High-Order Group-Velocity-Locked Vector Solitons. IEEE Photonics Journal, 2015, 7, 1-6.	2.0	18
264	Optical properties of Ho:YAG and Ho:LuAG polycrystalline transparent ceramics. Optical Materials Express, 2015, 5, 142.	3.0	18
265	Densification of zirconia doped yttria transparent ceramics using co-precipitated powders. Ceramics International, 2016, 42, 10770-10778.	4.8	18
266	High-resolution chalcogenide fiber bundles for longwave infrared imaging. Optics Express, 2017, 25, 26160.	3.4	18
267	3D Printing of Transparent Spinel Ceramics with Transmittance Approaching the Theoretical Limit. Advanced Materials, 2021, 33, e2007072.	21.0	18
268	Infrared optical properties of LaNiO3–platinized silicon and PbZrχTi1â^χO3–LaNiO3–platinized silicon heterostructures. Applied Physics Letters, 2001, 78, 793-795.	3.3	17
269	A Real Pivot Structure for MEMS Tunable Lasers. Journal of Microelectromechanical Systems, 2007, 16, 269-278.	2.5	17
270	Diode-pumped passively mode-locked Nd:CLNGG laser. Optics Communications, 2009, 282, 291-293.	2.1	17

#	Article	IF	CITATIONS
271	2.1 μm Ho:LuAG ceramic laser intracavity pumped by a diode-pumped Tm:YAG laser. Chinese Optics Letters, 2014, 12, 121405.	2.9	17
272	Infrared optical properties of amorphous hydrogenated carbon nitride film. Journal of Non-Crystalline Solids, 2000, 278, 213-217.	3.1	16
273	660GHz Solitons Source Based on Modulation Instability in Short Cavity. Optics Express, 2003, 11, 2480.	3.4	16
274	Diode-end-pumped passively mode-locked Nd:LuVO4 laser with a semiconductor saturable-absorber mirror. Applied Physics B: Lasers and Optics, 2008, 91, 425-428.	2.2	16
275	Fabrication and laser performance of highly transparent Nd:YAG ceramics from well-dispersed Nd:Y2O3 nanopowders by freeze-drying. Journal of Nanoparticle Research, 2011, 13, 3853-3860.	1.9	16
276	Multi-order Stokes output based on intra-cavity KTiOAsO_4 Raman crystal. Optics Express, 2014, 22, 19662.	3.4	16
277	Soliton-dark pulse pair formation in birefringent cavity fiber lasers through cross phase coupling. Optics Express, 2015, 23, 26252.	3.4	16
278	RbTiOPO4 cascaded Raman operation with multiple Raman frequency shifts derived by Q-switched Nd:YAlO3 laser. Scientific Reports, 2016, 6, 33852.	3.3	16
279	Yellow, lime and green emission selectable by BBO angle tuning in <i>Q</i> -switched Nd:YVO ₄ self-Raman laser. Laser Physics Letters, 2018, 15, 075803.	1.4	16
280	A 142 W Ho:YAG laser single-end-pumped by a Tm-doped fiber laser at 1931 nm. Laser Physics Letters, 2019, 16, 115001.	1.4	16
281	Fabrication and microstructures of YAG transparent ceramics. Science of Sintering, 2008, 40, 311-317.	1.4	16
282	Antiphase dynamics in an optically pumped bidirectional ring laser. Optics Communications, 1996, 126, 318-325.	2.1	15
283	Close spaced ultra-short bound solitons from DI-NOLM Figure-8 fiber laser. Optics Communications, 2003, 220, 297-302.	2.1	15
284	Diode end-pumped passively Q-switched Nd:YAG ceramic laser with Cr4+:YAG saturable absorber. Laser Physics, 2008, 18, 1508-1511.	1.2	15
285	A miniature tunable coupled-cavity laser constructed by micromachining technology. Applied Physics Letters, 2008, 92, 031105.	3.3	15
286	Diode-pumped passively mode-locked Nd:CaNb2O6 laser. Laser Physics, 2010, 20, 1331-1334.	1.2	15
287	High efficient diode-pumped passively mode-locked Nd:LuAG laser. Laser Physics Letters, 2012, 9, 406-409.	1.4	15
288	Fabrication and Optical Properties of Highly Transparent <scp>Er</scp> : <scp>YAG</scp> Polycrystalline Ceramics for Eye‧afe Solid‧tate Lasers". International Journal of Applied Ceramic Technology, 2013, 10, 123-128.	2.1	15

#	Article	IF	CITATIONS
289	Generation of 2-\$mu{m m}\$ Light Based on a Noncritical Phase Matching OPO Technique. IEEE Photonics Technology Letters, 2013, 25, 690-693.	2.5	15
290	251 fs pulse generation with a Nd ³⁺ -doped Ca ₃ Gd ₂ (BO ₃) ₄ disordered crystal. RSC Advances, 2015, 5, 44137-44141.	3.6	15
291	Initial conditions for dark soliton generation in normal-dispersion fiber lasers. Applied Optics, 2015, 54, 71.	1.8	15
292	Continuous-wave laser operation of Nd:LuAG ceramic with ^4F_3â^•2→^4I_11â^•2 transition. Optical Materials Express, 2015, 5, 611.	3.0	15
293	Low-level sintering aids for highly transparent Yb:Y2O3 ceramics. Journal of Alloys and Compounds, 2017, 695, 1414-1419.	5.5	15
294	Enhanced nonlinear optical responses of graphene in multi-frequency topological edge modes. Optics Express, 2019, 27, 32746.	3.4	15
295	298 fs passively mode-locked ring fiber soliton laser. Microwave and Optical Technology Letters, 2002, 32, 329-333.	1.4	14
296	Dynamic sideband generation in soliton fiber lasers. Optics Communications, 2007, 275, 213-216.	2.1	14
297	Room temperature diode-pumped Yb:CaYAlO4 laser with near quantum limit slope efficiency. Laser Physics Letters, 2011, 8, 193-196.	1.4	14
298	Lowâ€ŧemperature stimulated Raman scattering spectroscopy of tetragonal GdVO ₄ single crystals. Physica Status Solidi (B): Basic Research, 2014, 251, 1045-1062.	1.5	14
299	Watt-level broadly wavelength tunable mode-locked solid-state laser in the 2  μm water absorption region. Photonics Research, 2017, 5, 583.	7.0	14
300	27  μm optical vortex beam directly generated from an Er:Y ₂ O ₃ ceramic lase Optics Letters, 2019, 44, 4973.	er. 3.3	14
301	Fabrication of highâ€efficiency Yb:Y ₂ O ₃ laser ceramics without photodarkening. Journal of the American Ceramic Society, 2022, 105, 3375-3381.	3.8	14
302	Experimental control of single-mode laser chaos by using continuous, time-delayed feedback. Physical Review E, 1998, 57, 6596-6598.	2.1	13
303	Polarization-resolved study of diode-pumped passively Q-switched Nd:GdVO_4 lasers. Applied Optics, 2006, 45, 6792.	2.1	13
304	Multi-stage pulse compression by use of cascaded quadratic nonlinearity. Optics Communications, 2007, 273, 207-213.	2.1	13
305	Thermal-Optic Switch by Total Internal Reflection of Micromachined Silicon Prism. IEEE Journal of Selected Topics in Quantum Electronics, 2007, 13, 348-358.	2.9	13
306	Highly efficient continuous-wave Nd:YAG ceramic lasers at 946 nm. Laser Physics Letters, 2013, 10, 075802.	1.4	13

#	Article	IF	CITATIONS
307	Effects of Ho3+-doping concentration on the performances of resonantly pumped Ho:YAG ceramic lasers. Optical Materials, 2013, 35, 712-714.	3.6	13
308	Sub-100fs pulse generation in a diode pumped Yb:Sc2SiO5 laser. Optics Communications, 2013, 294, 237-240.	2.1	13
309	Passively Mode-Locked Tm:YAG Ceramic Laser Based on Graphene. IEEE Journal of Selected Topics in Quantum Electronics, 2015, 21, 50-55.	2.9	13
310	45-fs Diode-Pumped Passively Mode-Locked Yb:NaY(WO ₄) ₂ Soliton Laser. IEEE Photonics Technology Letters, 2016, 28, 1298-1301.	2.5	13
311	Application of a novel biomimetic double-ligand zirconium-based metal organic framework in environmental restoration and energy conversion. Journal of Colloid and Interface Science, 2022, 610, 136-151.	9.4	13
312	Ultraviolet-infrared optical properties of highly (100)-oriented LaNiO3 thin films on Pt–Ti–SiO2–Si wafer. Journal of Applied Physics, 2001, 90, 2699-2702.	2.5	12
313	Passive mode locking of ceramic Nd: YAG using (7,5) semiconducting single walled carbon nanotubes. Optical Materials, 2011, 33, 679-683.	3.6	12
314	Detection of microscope-excited surface plasmon polaritons with Rayleigh scattering from metal nanoparticles. Applied Physics Letters, 2013, 103, .	3.3	12
315	Resonantly pumped Q-switched Er:YAG ceramic laser at 1645 nm. Optics Express, 2014, 22, 24004.	3.4	12
316	Manipulating propagating graphene plasmons at near field by shaped graphene nano-vacancies. Journal of the Optical Society of America A: Optics and Image Science, and Vision, 2014, 31, 691.	1.5	12
317	Induced dark solitary pulse in an anomalous dispersion cavity fiber laser. Optics Express, 2015, 23, 28430.	3.4	12
318	Transparent Ceramic Materials. Topics in Mining, Metallurgy and Materials Engineering, 2015, , 29-91.	1.6	12
319	Gold Nanorods as Single and Combined Saturable Absorbers for a High-Energy <named-content content-type="math" xlink:type="simple"> <inline-formula> <tex-math notation="TeX">\$Q\$</tex-math </inline-formula>-Switched Nd:YAG Solid-State Laser. IEEE Photonics Journal. 2015. 7. 1-10.</named-content 	2.0	12
320	Highly stable self-pulsed operation of an Er:Lu ₂ O ₃ ceramic laser at 2.7 <i>µ</i> m. Laser Physics Letters, 2017, 14, 045803.	1.4	12
321	Unusual Evolutions of Dissipative-Soliton-Resonance Pulses in an All-Normal Dispersion Fiber Laser. IEEE Photonics Journal, 2019, 11, 1-9.	2.0	12
322	Vectorial Nature in Nonlinear Multimode Interference Based Ultrafast Fiber Lasers. IEEE Photonics Journal, 2020, 12, 1-10.	2.0	12
323	W-type normal dispersion thulium-doped fiber-based high-energy all-fiber femtosecond laser at 1.7  µm. Optics Letters, 2021, 46, 3637.	3.3	12
324	Polycrystalline alumina ceramic fabrication using digital stereolithographic light process. Ceramics International, 2021, 47, 33815-33826.	4.8	12

#	Article	IF	CITATIONS
325	Few-moded ultralarge mode area chalcogenide photonic crystal fiber for mid-infrared high power applications. Optics Express, 2020, 28, 16658.	3.4	12
326	Uniqueness of the chaotic attractor of a single-mode laser. Physical Review A, 1994, 49, 1296-1300.	2.5	11
327	Subtleties of the period-doubling chaos of an optically pumpedNH3single-mode ring laser. Physical Review A, 1995, 52, 717-725.	2.5	11
328	Energy quantization of twin-pulse solitons in a passively mode-locked fiber ring laser. Applied Physics B: Lasers and Optics, 2003, 77, 585-588.	2.2	11
329	Effective cavity dispersion shift induced by nonlinearity in a fiber laser. Physical Review A, 2009, 80, .	2.5	11
330	Diode-pumped femtosecond Yb:CaNb_2O_6 laser. Optics Letters, 2011, 36, 3888.	3.3	11
331	Efficient Graphene Q-Switching of an In-Band Pumped Polycrystalline Er:YAG Ceramic Laser at 1617 nm. IEEE Photonics Technology Letters, 2013, 25, 1294-1296.	2.5	11
332	Widely tunable, narrow bandwidth polycrystalline ceramic Er:YAG laser with a volume Bragg grating. Optics Express, 2014, 22, 7154.	3.4	11
333	Rapid Rate Sintering of Yttria Transparent Ceramics. Journal of the American Ceramic Society, 2016, 99, 1935-1942.	3.8	11
334	Revision on fiber dispersion measurement based on Kelly sideband measurement. Microwave and Optical Technology Letters, 2016, 58, 242-245.	1.4	11
335	CW and passively Q-switched laser performance of Nd:Lu2SiO5 crystal. Optical Materials, 2016, 51, 241-244.	3.6	11
336	Nanosecond Pulse Generation at 2.7 μm From a Passively Q-Switched Er:Y2O 3 Ceramic Laser. IEEE Journal of Selected Topics in Quantum Electronics, 2018, 24, 1-6.	2.9	11
337	Highly efficient CW operation of a diode pumped Nd:Y ₂ O ₃ ceramic laser. Optical Materials Express, 2018, 8, 3518.	3.0	11
338	Cavity-assisted modulation instability lasing of a fiber ring laser. Applied Physics B: Lasers and Optics, 2019, 125, 1.	2.2	11
339	Generation of sub-100-fs pulses from a diode-pumped Yb:Y3ScAl4O12 ceramic laser. Chinese Optics Letters, 2017, 15, 121403.	2.9	11
340	Selective frequency mixing in a cascaded self-Raman laser with a critical phase-matched LBO crystal. Journal of Luminescence, 2022, 244, 118698.	3.1	11
341	Observation of modulation instability in a fiber soliton ring laser. Optics Communications, 1999, 167, 125-128.	2.1	10
342	Numerical studies of routes to chaos in passively mode-locked fiber soliton ring lasers with dispersion-managed cavity. Europhysics Letters, 2005, 71, 56-62.	2.0	10

#	Article	IF	CITATIONS
343	Tunable dual-wavelength laser constructed by silicon micromachining. Applied Physics Letters, 2008, 92, 051113.	3.3	10
344	Inverse-Gaussian apodized fiber Bragg grating for dual-wavelength lasing. Applied Optics, 2010, 49, 1373.	2.1	10
345	Continuous-wave and Q-switched operation of a resonantly pumped polycrystalline ceramic Ho:LuAG laser. Optics Express, 2014, 22, 19014.	3.4	10
346	Dissipative soliton operation of a diode pumped Yb:NaY(WO_4)_2 laser. Optics Express, 2015, 23, 32311.	3.4	10
347	Cascaded Self-Raman Laser Emitting Around 1.2–1.3Â <italic>μ</italic> m Based on a c-cut Nd:YVO ₄ Crystal. IEEE Photonics Journal, 2017, 9, 1-7.	2.0	10
348	Yttria nanopowders with low degree of aggregation by a spray precipitation method. Ceramics International, 2018, 44, 20472-20477.	4.8	10
349	Fabrication and microstructural characterizations of lasing grade Nd:Y ₂ O ₃ ceramics. Journal of the American Ceramic Society, 2019, 102, 7462-7468.	3.8	10
350	Passively Q-switched multiple visible wavelengths switchable YVO4 Raman laser. Journal of Luminescence, 2020, 228, 117650.	3.1	10
351	Period doubling eigenstates in a fiber laser mode-locked by nonlinear polarization rotation. Optics Express, 2020, 28, 9802.	3.4	10
352	Narrow linewidth self-injection locked fiber laser based on a crystalline resonator in add-drop configuration. Optics Letters, 2022, 47, 1525.	3.3	10
353	Experimentally tracking unstable steady states by large periodic modulation. Physical Review E, 1998, 57, 397-401.	2.1	9
354	Miniaturized injection-locked laser using microelectromechanical systems technology. Applied Physics Letters, 2005, 87, 101101.	3.3	9
355	Period-doubling of multiple solitons in a passively mode-locked fiber laser. Optics Communications, 2007, 273, 554-559.	2.1	9
356	Passive harmonic mode locking of gain-guided solitons in erbium-doped fiber lasers. Science Bulletin, 2008, 53, 676-680.	1.7	9
357	Dynamics of gain-guided solitons in a dispersion-managed fiber laser with large normal cavity dispersion. Optics Communications, 2008, 281, 3324-3326.	2.1	9
358	Experimental observation of optical vortex in self-frequency-doubling generation. Applied Physics Letters, 2011, 99, 241102.	3.3	9
359	Dual-wavelength passively mode-locked Nd: GdVO4ÂlaserÂwithÂorthogonal polarizations. Applied Physics B: Lasers and Optics, 2011, 102, 775-779.	2.2	9
360	Growth, spectral properties, and laser demonstration ofÂNd:GYSO crystal. Applied Physics B: Lasers and Optics, 2011, 104, 53-58.	2.2	9

#	Article	IF	CITATIONS
361	Mode″ocked Yb:LuAG ceramics laser. Physica Status Solidi C: Current Topics in Solid State Physics, 2013, 10, 967-968.	0.8	9
362	High-power LD end-pumped Tm:YAG ceramic slab laser. Applied Physics B: Lasers and Optics, 2015, 118, 533-538.	2.2	9
363	Pump hysteresis and bistability of dissipative solitons in all-normal-dispersion fiber lasers. Applied Optics, 2015, 54, 3774.	2.1	9
364	Unidirectional dissipative soliton operation in an all-normal-dispersion Yb-doped fiber laser without an isolator. Applied Optics, 2015, 54, 7912.	2.1	9
365	High-Peak-Power Acousto-Optically Q-Switched Er:Y2O3 Ceramic Laser at â^¼2.7 μm. IEEE Photonics Journal, 2017, 9, 1-6.	2.0	9
366	Observation of vector solitons supported by third-order dispersion. Physical Review A, 2019, 99, .	2.5	9
367	Dual-wavelength dissipative solitons in an anomalous-dispersion-cavity fiber laser. Nanophotonics, 2020, 9, 2361-2366.	6.0	9
368	Anti-dark solitons in a single mode fiber laser. Physics Letters, Section A: General, Atomic and Solid State Physics, 2021, 395, 127226.	2.1	9
369	High Power Continuous-Wave and Graphene Q-switched Operation of Er:YAG Ceramic Lasers at ~1.6 ㎛. Journal of the Optical Society of Korea, 2013, 17, 5-9.	0.6	9
370	Direct generation of ultrafast vortex beam from a Tm:CaYAlO ₄ oscillator featuring pattern matching of a folded-cavity resonator. Optics Express, 2021, 29, 39312.	3.4	9
371	Fabrication and comprehensive structural and spectroscopic properties of Er:Y2O3 transparent ceramics. Journal of Rare Earths, 2022, 40, 1913-1919.	4.8	9
372	Recent progress on HgCdTe at the national laboratory for infrared physics in china. Journal of Electronic Materials, 1996, 25, 1176-1182.	2.2	8
373	High-power passive mode-locking of a diode pumped Yb:GdVO4 laser. Optics Communications, 2008, 281, 5382-5384.	2.1	8
374	A passively <i>Q</i> -switched Er:LuYAG laser with a graphene saturable absorber. Laser Physics Letters, 2013, 10, 105810.	1.4	8
375	Thermal, spectral and laser characteristics of Nd doped La0.05Lu0.95VO4 crystal. Journal of Crystal Growth, 2014, 387, 66-72.	1.5	8
376	Growth and characterization of large-scale Ti:sapphire crystal using heat exchange method for ultra-fast ultra-high-power lasers. CrystEngComm, 2015, 17, 2801-2805.	2.6	8
377	Period-Timing Bifurcations in a Dispersion-Managed Fiber Laser With Zero Group Velocity Dispersion. IEEE Photonics Journal, 2016, 8, 1-8.	2.0	8
378	Breach and recurrence of dissipative soliton resonance during period-doubling evolution in a fiber laser. Physical Review A, 2020, 102, .	2.5	8

#	Article	IF	CITATIONS
379	Exploring the evolution of pores in HIPed Y2O3 transparent ceramics. Ceramics International, 2021, 47, 11637-11643.	4.8	8
380	Helical-wave emission of lasers. Journal of the Optical Society of America B: Optical Physics, 1994, 11, 2089.	2.1	7
381	Soliton shaping of dispersive waves in a passively mode-locked fibre soliton ring laser. Optical and Quantum Electronics, 2001, 33, 1139-1147.	3.3	7
382	Bound solitons with 103-fs pulse width and 585.5-fs separation from DI-NOLM figure-8 fiber laser. Microwave and Optical Technology Letters, 2003, 39, 163-164.	1.4	7
383	Development of Translucent Oxyapatite Ceramics by Spark Plasma Sintering. Journal of the American Ceramic Society, 2010, 93, 3060-3063.	3.8	7
384	Wavelength-tunable picosecond soliton fiber laser with Topological Insulator: Bi_2Se_3 as a mode locker: erratum. Optics Express, 2013, 21, 444.	3.4	7
385	Compact single-frequency Tm:YAG ceramic laser with a volume Bragg grating. Laser Physics Letters, 2013, 10, 075805.	1.4	7
386	Mode locking of Yb:GdYAG ceramic lasers with an isotropic cavity. Laser Physics Letters, 2013, 10, 095702.	1.4	7
387	Dissipative vector soliton in a dispersion-managed fiber laser with normal dispersion. Applied Optics, 2014, 53, 8216.	2.1	7
388	A modified model for the LD pumped 2μm Tm:YAG laser: Thermal behavior and laser performance. Optics Communications, 2014, 332, 332-338.	2.1	7
389	Passively Q-switched 1617-nm polycrystalline ceramic Er:YAG laser using a Cr:ZnSe saturable absorber. Applied Physics B: Lasers and Optics, 2015, 120, 305-309.	2.2	7
390	Impulsive stimulated Raman scattering in tetragonal GdVO ₄ single crystal: many-phonon Stokes and cross-cascaded lasing. Laser Physics Letters, 2015, 12, 085801.	1.4	7
391	Efficient Nd:YAGâ^–KTiOAsO 4 cascaded Raman laser emitting around 1.2Âμ4m. Optical Materials, 2017, 71, 66-69.	3.6	7
392	Peak-Power-Clamped Passive Q-Switching of a Thulium/Holmium Co-Doped Fiber Laser. Journal of Lightwave Technology, 2018, 36, 4975-4980.	4.6	7
393	Excitation of graphene magneto-plasmons in terahertz range and giant Kerr rotation. Journal of Applied Physics, 2019, 125, .	2.5	7
394	High Peak Power Acousto-Optically Q-Switched Ho:Y ₂ O ₃ Ceramic Laser at 2117 nm. IEEE Photonics Technology Letters, 2020, 32, 492-495.	2.5	7
395	Dark-bright soliton trapping in a fiber laser. Optics Letters, 2021, 46, 1105.	3.3	7
396	Collision between soliton and polarization domain walls in fiber lasers. Optics Express, 2021, 29, 12590.	3.4	7

#	Article	IF	CITATIONS
397	Noise-like pulses with an h-shape from a 2 <i>î¼</i> m semiconductor saturable-absorber mirror mode-locked fiber oscillator. Laser Physics Letters, 2020, 17, 115101.	1.4	7
398	Single longitudinal mode lasing near the exceptional point in a fiber laser using a tunable isolator. Optics Letters, 2022, 47, 2222.	3.3	7
399	Phase dynamics of a detuned single-mode laser. Applied Physics B, Photophysics and Laser Chemistry, 1992, 55, 104-108.	1.5	6
400	Phase-dependent helical pattern formation in a laser. Optics Communications, 1995, 114, 95-100.	2.1	6
401	High-power diode-end-pumped CW Nd:GdVO4 laser. Optics and Laser Technology, 2005, 37, 51-54.	4.6	6
402	A highly efficient diode-pumped passively mode-locked Nd:Lu _{1.5} Y _{1.5} Al ₅ O ₁₂ laser. Laser Physics Letters, 2013, 10, 095801.	1.4	6
403	Continuous-Wave and Q-Switched Neodymium-Doped Yttrium Aluminum Garnet Ceramic Laser at 1356 nm Single Wavelength. Applied Physics Express, 2013, 6, 022705.	2.4	6
404	Orthorhombic YAlO ₃ – a novel manyâ€phonon SRSâ€active crystal. Laser and Photonics Reviews, 2014, 8, 904-915.	8.7	6
405	Q-switched mode locking of a fiber laser resonantly pumped Er:YAG ceramic laser at 1645 nm using graphene as saturable absorber. Journal of Nonlinear Optical Physics and Materials, 2015, 24, 1550001.	1.8	6
406	Eye-safe Nd:LuAG ceramic lasers. Optical Materials Express, 2017, 7, 1374.	3.0	6
407	Short-Pulse-Width Repetitively Q-Switched ~2.7-μm Er:Y2O3 Ceramic Laser. Applied Sciences (Switzerland), 2017, 7, 1201.	2.5	6
408	Vector dark solitons in a single mode fibre laser. Laser Physics Letters, 2019, 16, 085110.	1.4	6
409	Microfiber-Knot-Resonator-Induced Energy Transferring From Vector Noise-Like Pulse to Scalar Soliton Rains in an Erbium-Doped Fiber Laser. IEEE Journal of Selected Topics in Quantum Electronics, 2021, 27, 1-6.	2.9	6
410	Power scaling of diode-pumped Er:Y ₂ O ₃ ceramic laser at 2.7 μm. Applied Physics Express, 2022, 15, 062004.	2.4	6
411	Spontaneous self-organisation in chaotic laser mode-mode interaction. Optics Communications, 1996, 131, 89-94.	2.1	5
412	Mechanism of bound soliton pulse formation in a passively mode locked fiber ring laser. Optical Engineering, 2002, 41, 2778.	1.0	5
413	Periodic soliton amplitude variation caused by unstable dispersive waves in a laser. Optics Communications, 2005, 254, 242-247.	2.1	5
414	Soliton in fiber lasers beyond the Cinzburg–Landau equation approximation. Optics Communications, 2007, 275, 404-408.	2.1	5

#	Article	IF	CITATIONS
415	Diode-pumped femtosecond passively mode-locked Yb:LPS laser. Laser Physics Letters, 2012, 9, 726-729.	1.4	5
416	A compact, CW mid-infrared intra-cavity Nd:Lu0.5Y0.5VO4â^—KTA-OPO at 3.5 μm. Laser Physics Letters, 2013, 10, 055803.	1.4	5
417	Passive mode-locking performance of mixed Nd:La_011Y_089VO_4 crystal. Optics Express, 2014, 22, 5350.	3.4	5
418	Highly efficient resonantly pumped 2000Ânm Tm:YAG ceramic laser. Optical Engineering, 2014, 53, 040501.	1.0	5
419	Bound States of Vector Dissipative Solitons. IEEE Photonics Journal, 2015, 7, 1-8.	2.0	5
420	Self-Pulsed Nanosecond 2.7- <named-content content-type="math" xlink:type="simple"> <inline-formula> <tex-math notation="LaTeX">\$muext{m}\$</tex-math </inline-formula></named-content> Solid-State Erbium Laser by Cooperatively Enhanced Reabsorption. IEEE Photonics Journal, 2015, 7, 1-7.	2.0	5
421	Nd:(Gd0.3Y0.7)2SiO5 crystal: A novel efficient dual-wavelength continuous-wave medium. Optics Communications, 2016, 366, 77-80.	2.1	5
422	Mid-Infrared Tunable Intracavity Singly Resonant Optical Parametric Oscillator Based on MgO:PPLN. International Journal of Optics, 2017, 2017, 1-5.	1.4	5
423	High-Power Ho-Doped Sesquioxide Ceramic Laser In-Band Pumped by a Tm-Doped All-Fiber MOPA. IEEE Photonics Journal, 2018, 10, 1-7.	2.0	5
424	Fabrication of laser grade Yb: Y2O3 transparent ceramics with ZrO2 additive through hot isostatic pressing. Materials Today Communications, 2020, 24, 101185.	1.9	5
425	Period doubling of multiple dissipative-soliton-resonance pulses in a fibre laser. OSA Continuum, 2020, 3, 911.	1.8	5
426	Local nonlinearity engineering of evanescent-field-interaction fiber devices embedding in black phosphorus quantum dots. Nanophotonics, 2021, 11, 87-100.	6.0	5
427	Ultrafast Tm:CaYAlO4 laser with pulse regulation and saturation parameters evolution in the 2Âl¼m water absorption band. Optics and Laser Technology, 2022, 152, 108096.	4.6	5
428	Antiphase dynamics of a chaotic multimode laser. Physical Review A, 1997, 56, 1050-1052.	2.5	4
429	Determination of cut-off wavelength and composition distribution in Hg1-xCdxTe. Journal of Electronic Materials, 1998, 27, 718-721.	2.2	4
430	Self-started unidirectional operation of a fibre ring soliton laser without an isolator. Journal of Optics, 2007, 9, 477-479.	1.5	4
431	Diode-pumped passively Q-switched Nd:YAG ceramic laser with GaAs saturable absorber. Journal of Optics, 2007, 9, 621-625.	1.5	4
432	Ultrashort pulse generation in lasers by nonlinear pulse amplification and compression. Applied Physics Letters, 2007, 90, 051102.	3.3	4

#	Article	IF	CITATIONS
433	Diode-end-Pumped Nd:YAG Ceramic and Crystal Operation at 1,123Ânm. Journal of Russian Laser Research, 2013, 34, 458-462.	0.6	4
434	Controlled Generation of Bright or Dark Solitons in a Fiber Laser by Intracavity Nonlinear Absorber. IEEE Photonics Journal, 2016, 8, 1-12.	2.0	4
435	Orthogonally dual-polarization passively mode-locking operation of Nd:La0.25Gd0.75VO4 crystal. Optics and Laser Technology, 2016, 85, 60-65.	4.6	4
436	1.96-μm Tm:YAG Ceramic Laser. IEEE Photonics Journal, 2017, 9, 1-7.	2.0	4
437	Broadband features of passively harmonic mode locking in dispersion-managed erbium-doped all-fiber lasers. Optics Communications, 2018, 416, 5-9.	2.1	4
438	High Power and Short Pulse Width Operation of Passively Q-Switched Er:Lu2O3 Ceramic Laser at 2.7 μm. Applied Sciences (Switzerland), 2018, 8, 801.	2.5	4
439	The phase, microstructure evolution and the Nd3+ function in the fabrication process of LuAG transparent ceramics. Journal of the European Ceramic Society, 2018, 38, 4043-4049.	5.7	4
440	Fabrication and rheological behavior of tapeâ€casting slurry for ultraâ€thin multilayer transparent ceramics. International Journal of Applied Ceramic Technology, 2020, 17, 1255-1263.	2.1	4
441	Stable Q-switched mode-locking of Er:YAG ceramic laser at 1645 nm using a semiconductor saturable absorber. Japanese Journal of Applied Physics, 2020, 59, 072003.	1.5	4
442	Synthesis of yttria nanopowder with poly acrylic acid as dispersant for highly transparent yttria ceramics. Journal of the American Ceramic Society, 2022, 105, 2029-2037.	3.8	4
443	1ÂkHz, 1.5ÂMW peak power pulse generation from an acousto-optically Q-switched Ho:GdVO4 oscillator. Optics and Laser Technology, 2022, 152, 108114.	4.6	4
444	Optical "friction wheels†asymmetric seeding of the TEM01 hybrid mode of a HeNe laser. Optics Communications, 1994, 105, 320-324.	2.1	3
445	The optical field of type-III intermittent pulsing of a single mode laser. Physics Letters, Section A: General, Atomic and Solid State Physics, 1995, 202, 363-368.	2.1	3
446	Growth and Q-switching performance on mixed laser crystal Nd0.0055(Gd0.64Y0.36)0.9945VO4. Journal of Crystal Growth, 2005, 281, 508-512.	1.5	3
447	PERIOD-DOUBLING ROUTE TO CHAOS IN DIODE-PUMPED PASSIVELY Q-SWITCHED Nd:GdVO4 AND Nd:YVO4 LASERS. International Journal of Bifurcation and Chaos in Applied Sciences and Engineering, 2006, 16, 2689-2696.	1.7	3
448	Graphene mode locked ultrafast fiber lasers. , 2011, , .		3
449	DISSIPATIVE SOLITON OPERATION OF AN Yb³⁺ : Sc₂SiO₅ LASER IN THE VICINITY OF ZERO GROUP VELOCITY DISPERSION. Optics and Photonics Letters, 2012, 05, 1250001.	0.8	3
450	Fabrication and Spectroscopic Properties of Transparent Yb:YAG Laser Ceramics. Solid State Phenomena, 0, 185, 44-47.	0.3	3

#	Article	IF	CITATIONS
451	Fabrication and Upconversion Luminescence of Highly Transparent Er:YAG Ceramics. Solid State Phenomena, 0, 185, 55-59.	0.3	3
452	Ceramic Powder Synthesis. Topics in Mining, Metallurgy and Materials Engineering, 2015, , 93-189.	1.6	3
453	Energy level systems and transitions of Ho:LuAG laser resonantly pumped by a narrow line-width Tm fiber laser. Optics Express, 2016, 24, 27536.	3.4	3
454	A Diode-Pumped Dual-Wavelength Tm, Ho:ÂYAG Ceramic Laser. IEEE Photonics Journal, 2016, 8, 1-7.	2.0	3
455	Diode-pumped Nd:LuAG ceramic laser on 4 F 3/2 - 4 I 13/2 transition. Optical Materials, 2017, 71, 121-124.	3.6	3
456	Passive Q-switching of â^1⁄42.7 µm Er:Lu2O3ceramic laser with a semiconductor saturable absorber mirror. Japanese Journal of Applied Physics, 2018, 57, 022701.	1.5	3
457	Stable Q-Switched Mode-Locking of 2.7 μm Er:Y2O3 Ceramic Laser Using a Semiconductor Saturable Absorber. Applied Sciences (Switzerland), 2018, 8, 1155.	2.5	3
458	2 <i>µ</i> m vector mode-locked pulses from Tm:Y ₂ O ₃ ceramics laser. Laser Physics, 2019, 29, 045301.	1.2	3
459	Dissipative peregrine solitons in fiber lasers. JPhys Photonics, 2020, 2, 034011.	4.6	3
460	Periodic power variation induced sideband instability in a single mode fiber laser. Laser Physics Letters, 2020, 17, 095103.	1.4	3
461	Polarization domain splitting and incoherently coupled dark-bright vector soliton formation in single mode fiber lasers. Journal of the Optical Society of America B: Optical Physics, 2021, 38, 24.	2.1	3
462	Coherently coupled vector black solitons in a quasi-isotropic cavity fiber laser. Optics Letters, 2020, 45, 6563.	3.3	3
463	High-power 1640â€nm Er:Y ₂ O ₃ ceramic laser at room temperature. Optics Letters, 2022, 47, 246.	3.3	3
464	Chaotic dynamics of an optically pumped NH_3 multitransverse-mode ring laser. Journal of the Optical Society of America B: Optical Physics, 1996, 13, 2055.	2.1	2
465	Homoclinic orbits and chaos in a multimode laser. Journal of the Optical Society of America B: Optical Physics, 1997, 14, 2930.	2.1	2
466	Dependence of transient dynamics in a class-C laser upon variation of inversion with time. Physical Review A, 1998, 57, 559-566.	2.5	2
467	Observation of spectral enhancement in a soliton fiber laser with fiber Bragg grating. Optics Express, 2009, 17, 3508.	3.4	2
468	Inverse-Gaussian apodized fiber Bragg grating for microwave generation. , 2010, , .		2

#	Article	IF	CITATIONS
469	Bound solitons operation of a fiber laser mode-locked by carbon nanotubes. , 2010, , .		2
470	Fabrication and Properties of High Quality Transparent Ho:YAG Ceramics. Solid State Phenomena, 0, 185, 51-54.	0.3	2
471	Periodic dark pulse emission induced by delayed feedback in a quantum well semiconductor laser. AIP Advances, 2012, 2, 042157.	1.3	2
472	Highly Efficient Tm-Doped Yttrium Aluminum Garnet Ceramic Laser Based on the Novel Fiber-Bulk Hybrid Configuration. Applied Physics Express, 2013, 6, 092107.	2.4	2
473	Optical properties and laser performance of Ho:LuAG ceramics. Physica Status Solidi C: Current Topics in Solid State Physics, 2013, 10, 903-906.	0.8	2
474	Vector gain-guided dissipative solitons in a net normal dispersive fiber laser. IEEE Photonics Technology Letters, 2016, , 1-1.	2.5	2
475	Short pulse-width gain-switched Ho:YAG ceramic laser at â^¼209  μm. Applied Optics, 2016, 55, 1890.	2.1	2
476	Temporal vector cavity solitons in a net anomalous dispersion fiber laser. Laser Physics Letters, 2016, 13, 025103.	1.4	2
477	Stable Q-switched mode-locking of an in-band pumped Ho : Y ₂ O ₃ ceramic laser at 2117 nm. Quantum Electronics, 2021, 51, 419-422.	1.0	2
478	Effects of glycerol addition on the slurry dispersion and mechanical properties of alumina ceramics prepared by gel-casting process. Ceramics International, 2021, 47, 20260-20267.	4.8	2
479	21-fs Kerr-lens Mode-locked Yb:CaYAlO4 Laser. , 2018, , .		2
480	Adaptive genetic algorithm-based 2 μm intelligent mode-locked fiber laser. OSA Continuum, 2021, 4, 2747.	1.8	2
481	Stability of the change of the third-order nonlinearity in silica fibre. , 0, , .		1
482	GaAs wafer for passive mode locking and compression of energetic Q-switched pulses. Journal of Crystal Growth, 2006, 288, 162-165.	1.5	1
483	MEMS Tunable Dual-Wavelength Laser with Large Tuning Range. , 2007, , .		1
484	Passively Q-switched Nd:YAG ceramic laser with GaAs saturable absorber. , 2007, , .		1
485	Evidence of High-Order Vector Dissipative Soliton in a Fiber Laser. , 2010, , .		1
486	Atomic multi-layer graphene for dissipative soliton generation in Ytterbium-doped fiber laser. , 2010, , .		1

#	Article	IF	CITATIONS
487	Yb: <scp>YAG</scp> ceramics application for high energy cryogenic disk amplifier development. Physica Status Solidi (A) Applications and Materials Science, 2013, 210, 1232-1234.	1.8	1
488	Response to "Comment on â€~Ultra-short pulse generation by a topological insulator based saturable absorber'―[Appl. Phys. Lett. 103, 106101 (2013)]. Applied Physics Letters, 2013, 103, 106102.	3.3	1
489	Highly controllable optical bistability effect in a 2 μm Tm:YAG ceramic laser at room temperature. Optics Express, 2015, 23, 7619.	3.4	1
490	High repetition rate gain-switched Er:YAG ceramic laser at 1645 nm. Laser Physics, 2016, 26, 025804.	1.2	1
491	In-band pumped Q-switched polycrystalline Er:YAG ceramic laser at 1617 and 1634Ânm. Optical Materials, 2017, 71, 9-12.	3.6	1
492	Evolution from Periodic Intensity Modulations to Dissipative Vector Solitons in A Single-Mode Fiber Laser. Photonics, 2020, 7, 103.	2.0	1
493	Optical properties of transparent ZnSe0.9S0.1 mixed crystal ceramics prepared by hot isostatic pressing. Optical Materials, 2020, 108, 110214.	3.6	1
494	Dark solitons embedded in a stable periodic pulse train emitted by a fiber ring laser. JPhys Photonics, 2020, 2, 034009.	4.6	1
495	High Power Single Frequency Tm:Y ₂ O ₃ Ceramic Laser at 2015 nm. IEEE Photonics Journal, 2021, 13, 1-7.	2.0	1
496	Semiconductor Saturable Absorber Mirror Q-switched Er:Y2O3 Ceramic Laser at 2.7 \hat{l} ¼m. , 2017, , .		1
497	High-energy Pulse Generation at 1.76 μm from All-fiber Laser Configuration using Normal Dispersion Thulium-doped Fiber. , 2020, , .		1
498	Fabrication of high efficiency sesquioxide-based laser ceramics. , 2019, , .		1
499	High Power Diode-Pumped Er:Y2O3 Ceramic Laser at 2.7 ŵm. , 2021, , .		1
500	Self-steepening effect of optical pulse propagating in kerr medium. Microwave and Optical Technology Letters, 1988, 1, 340-343.	1.4	0
501	Helical wave laser as an "optical transistor― Optics Communications, 1997, 135, 305-309.	2.1	Ο
502	Incoherent-to-coherent conversion by use of the photorefractive beam-fanning effect and amplification by two-wave coupling in a photorefractive Ba_1-xSr_xTiO_3 crystal. Applied Optics, 2001, 40, 687.	2.1	0
503	Generalized Synchronization of Chaos in a Laser. AIP Conference Proceedings, 2002, , .	0.4	Ο
504	Relationship between thermally induced lensing and output power for a high-power laser-diode side-pumped solid-state laser. Microwave and Optical Technology Letters, 2004, 42, 361-365.	1.4	0

#	Article	IF	CITATIONS
505	Soliton interaction in a fiber ring laser. , 2005, 5623, 652.		Ο
506	Gain-guided and dispersion-managed soliton fiber lasers. , 2006, , .		0
507	Application of support vector machine for trace gas detection by using temperature-tuning optical parametric oscillator. , 2006, , .		Ο
508	Trace-gas detection based on the temperature-tuning periodically poled MgO: LiNbO 3 optical parametric oscillator. , 2006, 6379, 39.		0
509	Nanosecond square pulse generation in normal dispersion fiber ring lasers. , 2006, , .		Ο
510	Coexistence and competition between different soliton shaping mechanisms in a laser. , 2007, , .		0
511	Diode-end-pumped passively Q-switched Nd:YAG ceramic laser. , 2007, , .		0
512	Ultra-flat spectrum, multiwavelength operation in an erbium-doped fiber laser using power-clamping effect. , 2007, , .		0
513	Multi-pulse dispersion-managed solitons in a fiber laser at near zero dispersion. , 2007, , .		Ο
514	Application of ultra-flat spectrum multiwavelength EDFL in microwave photonic filters. , 2007, , .		0
515	Real Pivot Mechanism of Rotary Comb-Drive Actuators for MEMS Continuously Tunable Lasers. , 2007, ,		0
516	Passive harmonic mode locking of soliton bunches in a fiber ring laser. , 2007, , .		0
517	Vector soliton fiber lasers. , 2009, , .		0
518	Study on ultrafast disordered crystal lasers. , 2010, , .		0
519	Passive femtosecond mode-locking and cw laser performances of Yb ³⁺ : Sc <inf>2</inf> SiO <inf>5</inf> ., 2010, , .		0
520	The Nd:CaYAlO ₄ passively mode locked laser with a SESAM. , 2010, , .		0
521	Dark pulse emission from a 780nm diode laser with external cavity feedback. , 2011, , .		0
522	Diode-pumped passively mode-locked Yb:LPS laser. , 2011, , .		0

#	Article	IF	CITATIONS
523	Transient process of dissipative soliton generation in normal dispersion fiber lasers. , 2013, , .		Ο
524	Dark soliton operation fiber lasers. , 2013, , .		0
525	High power Tm:Fiber laser and in-band pumped Ho-doped ceramic lasers. , 2013, , .		0
526	Highly efficient passive mode locking of Nd:Lu2.9Gd0.1Al5O12garnet crystal. Laser Physics, 2013, 23, 055803.	1.2	0
527	Widely Tunable Tm:YAG Ceramic Laser With Volume Bragg Gratings. , 2014, , .		0
528	Low dimension structures and devices for new generation photonic technology. , 2014, , .		0
529	Soliton trapping in a Tm fiber laser. , 2014, , .		0
530	Bound states of vector dissipative solitons in normal dispersion fiber lasers. , 2014, , .		0
531	Special Section Guest Editorial: Laser Sensing and Imaging. Optical Engineering, 2014, 53, 061601.	1.0	0
532	Dissipative-soliton-resonance in all-normal-dispersion fiber lasers. , 2015, , .		0
533	Sintering and Densification of Transparent Ceramics. Topics in Mining, Metallurgy and Materials Engineering, 2015, , 467-517.	1.6	0
534	Laser Applications. Topics in Mining, Metallurgy and Materials Engineering, 2015, , 581-674.	1.6	0
535	Dissipative Soliton Operation and Features in Mode-locked Solid-state Lasers. , 2015, , .		0
536	Gain-switched Ho:YAG ceramic laser with an acousto-optic modulator. Optical Engineering, 2016, 55, 046115.	1.0	0
537	Broadband passive harmonic mode locking in a dispersion-managed Er-doped fiber laser. , 2017, , .		0
538	Introduction to the Special Issue on Fiber Lasers. IEEE Journal of Selected Topics in Quantum Electronics, 2018, 24, 1-2.	2.9	0
539	Rare-Earth Doped Sesquioxide Ceramics for Highly Efficient Mid-Infrared Lasers. , 2019, , .		0
540	Tunable Mode-Locked Fiber Laser in 1750–1870nm by Bending Normal Dispersion Thulium-Doped Fiber as		0

a Distribution Filter. , 2019, , .

#	Article	IF	CITATIONS
541	All-fiber High-energy 174 fs Laser at 1.78 μm using parabolic W-type Normal Dispersion Thulium-doped Fiber. , 2021, , .		0
542	Twin-pulse soliton emission of a passively mode-locked fiber ring laser. , 2003, , .		0
543	Group period-doubling of solitons in a fiber ring laser. , 2006, , .		0
544	Dynamics of gain-guided solitons in a fiber laser. , 2007, , .		0
545	Coexistence of Scalar Dissipative Solitons along Different Polarization Axes in a Highly Birefringent Fiber Laser with SESAM. , 2010, , .		0
546	Diode-pumped mode-locked Tm:YAG ceramic laser. , 2013, , .		0
547	Resonantly pumped Q-switched Ho:YAG ceramic laser. , 2013, , .		0
548	Narrow Gap Semiconductors. , 1998, , .		0
549	Cavity solitons in fiber lasers. , 2015, , .		0
550	Compression of dissipative-soliton-resonance pulses in a mode-locked fiber laser with a nonlinear optical loop mirror. , 2016, , .		0
551	High-peak-power and Short-pulse-width Actively Q-switched Er:Y2O3 Ceramic Lasers at ~2.7 μm. , 2017, , .		0
552	Nd:Y2O3 Transparent Ceramics: Fabrication and Laser Performance. , 2019, , .		0
553	High Power and Efficient Operation of Tm:YAG Ceramic Laser Resonantly Pumped at 1620 nm. IEEE Photonics Journal, 2022, 14, 1-3.	2.0	0
554	Efficiency degradation of laser ceramics caused by inappropriate dispersants and sintering aids. Optical Materials, 2021, 122, 111789.	3.6	0
555	Tm:Y2O3 ceramic laser in-band pumped at 1620 nm. , 2021, , .		Ο